

# Numerical Simulation of Contactless Methods for Measuring $j_C$ in High-Temperature Superconducting Film: Influence of Defect on Resolution and Accuracy<sup>\*)</sup>

Teruou TAKAYAMA, Atsushi KAMITANI, Soichiro IKUNO<sup>1)</sup> and Hiroaki NAKAMURA<sup>2)</sup>

*Yamagata University, 4-3-16 Johnan, Yonezawa, Yamagata 992-8510, Japan*

<sup>1)</sup>*Tokyo University of Technology, 1404-1 Katakura, Hachioji, Tokyo 192-0982, Japan*

<sup>2)</sup>*National Institute for Fusion Science, 322-6 Oroshi-cho, Toki 509-5292, Japan*

(Received 18 November 2013 / Accepted 13 March 2014)

The inductive method for measuring the critical current density in a high-temperature superconducting (HTS) film has been reproduced numerically. To this end, a numerical code has been developed for analyzing the time evolution of a shielding current density in an HTS film containing a crack. The computational results show that the accuracy of the inductive method monotonously increases with the height of the coil. In addition, the accuracy is slightly improved by changing the inner radius of the coil, and there exists the optimum inner radius. Although the accuracy is degraded due to the crack, this result means that the inductive method can be applied to the crack detection. Consequently, the crack located near the film edge cannot be detected with high accuracy because the crack is treated the same as the film edge.

© 2014 The Japan Society of Plasma Science and Nuclear Fusion Research

Keywords: critical current density, crack detection, high-temperature superconductor, inductive method, numerical simulation

DOI: 10.1585/pfr.9.3401129

## 1. Introduction

As is well known, a critical current density  $j_C$  is one of the most important parameters for engineering applications of high-temperature superconductors (HTSs). The standard four-probe method [1] has generally been employed for measuring  $j_C$ . In this method, the procedure is as follows: first, a large-area pad has to be coated with gold or silver to reduce the contact resistance between the HTS sample and the current lead. Next, the metallic coating requires the heat process. However, heating may destroy a sample surface or degrade superconducting characteristics. For this reason, contactless methods have been so far desired for measuring  $j_C$ .

For measuring  $j_C$  in an HTS film contactlessly, Claassen *et al.* have proposed the inductive method [2]. By applying an ac current  $I(t) = I_0 \sin 2\pi ft$  to a small coil placed just above an HTS film, they monitored a harmonic voltage induced in the coil. They found that, only when a coil current  $I_0$  exceeds a threshold current  $I_T$ , the third-harmonic voltage develops suddenly. They conclude that  $j_C$  can be evaluated from  $I_T$ . In contrast, Mawatari *et al.* elucidated the inductive method on the basis of the critical state model [3]. From their results, they derived a theoretical formula between  $j_C$  and  $I_T$ . The inductive method has been successfully employed as the measurement of the  $j_C$ -distributions and the detection of a crack [4].

author's e-mail: takayama@yz.yamagata-u.ac.jp

<sup>\*)</sup> This article is based on the presentation at the 23rd International Toki Conference (ITC23).

The purpose of the present study is to develop a numerical code for analyzing the time evolution of the shielding current density in an HTS film containing a crack and to investigate the influence of a coil shape on the accuracy of the inductive method. In addition, we investigate the influence of the film edge on the crack detection.

## 2. Governing Equations and Numerical Method

In Fig. 1, we show a schematic view of an inductive method. A small  $M$ -turn coil of outer radius  $R$ , inner radius  $R_{in}$ , and height  $H$  is placed just above a squared-shaped HTS film of length  $a$  and thickness  $b$ . An ac current  $I(t) = I_0 \sin 2\pi ft$  flows in the coil. Also, we define a distance  $L$  between the coil bottom and the film surface.

A square cross-section of the film is denoted by  $\Omega$ , and the outer boundary of  $\Omega$  is represented by  $C_0$ . We assume that a crack is included in  $\Omega$  and its shape is given by an inner boundary  $C_1$ . Moreover, a normal unit vector and a tangential unit vector on  $C_1$  are denoted by  $\mathbf{n}$  and  $\mathbf{t}$ , respectively.

We adopt the Cartesian coordinate system  $\langle O : \mathbf{e}_x, \mathbf{e}_y, \mathbf{e}_z \rangle$ , where  $z$ -axis is along the thickness direction, and the origin  $O$  is the centroid of the film. In order to determine the coil position, the symmetrical axis of the coil is shown by  $(x, y) = (x_A, y_A)$ .

A shielding current density  $\mathbf{j}$  in an HTS is closely related to the electric field  $\mathbf{E}$ . The relation can be written as

$\mathbf{E} = E(|\mathbf{j}|)[\mathbf{j}/|\mathbf{j}|]$  where a function  $E(j)$  is given by the power law:  $E(j) = E_c [j/j_c]^N$ . Here,  $E_c$  is the critical electric field, and  $N$  is a constant.

As is well known, the YBCO superconductors have a strong crystallographic anisotropy: the current flow in the  $c$ -axis direction differs from that in the  $ab$ -plane, and the flow along  $c$ -axis is almost negligible. Here, the  $c$ -axis is the direction along  $z$ , and it is perpendicular to the  $ab$ -plane. On the basis of the fact, we assume the thin-layer approximation [5]. Since the thickness of the HTS film is sufficiently thin that the shielding current density can hardly flow in the thickness direction.

Under the above assumptions, a shielding current density  $\mathbf{j}$  can be written as  $\mathbf{j} = (2/b)\nabla S \times \mathbf{e}_z$ , and the time evolution of the scalar function  $S(\mathbf{x}, t)$  is governed by the following integro-differential equation [5]:

$$\mu_0 \partial_t (\hat{W}S) + \partial_t \langle \mathbf{B} \cdot \mathbf{e}_z \rangle + (\nabla \times \mathbf{E}) \cdot \mathbf{e}_z = 0. \quad (1)$$

Here, a bracket  $\langle \rangle$  denotes an average operator over the thickness of the film, and  $\mathbf{E}$  is an electromagnetic field.  $\hat{W}S$  is defined by  $\hat{W}S \equiv \iint_{\Omega} Q(|\mathbf{x} - \mathbf{x}'|)S(\mathbf{x}', t)d^2\mathbf{x}' + (2/b)S(\mathbf{x}, t)$ , where both  $\mathbf{x}$  and  $\mathbf{x}'$  are position vectors in the  $xy$ -plane. The explicit form of  $Q(r)$  is described in [5].

The initial condition to (1) is given by  $S = 0$  at  $t = 0$ , and boundary conditions are assumed as follows:

$$S = 0, \text{ on } C_0, \quad (2)$$

$$\partial S / \partial s = 0, \text{ on } C_1, \quad (3)$$

$$h[\mathbf{E}] \equiv \oint_{C_1} \mathbf{E} \cdot \mathbf{t} ds = 0. \quad (4)$$

Here,  $s$  is an arclength along  $C_1$ . In this study, we assume that the surface area of the crack is equal to zero, and the crack passes through in the thickness direction of a film.

The boundary condition (4) is the integral form of Faraday's law. By applying the finite element method and the backward Euler method to the initial-boundary-value problem of (1), the problem is reduced to the nonlinear boundary-value problem. By using the Newton method, it is transformed by simultaneous linear equations. Note that  $h[\mathbf{E}]$  does not vanish numerically. This is mainly because the boundary condition (4) is included in the weak form by discretizing the initial-boundary-value problem of (1). For this reason, we adopt the virtual voltage method [6] proposed by Kamitani *et al.* Under a numerical method, a numerical code is developed for analyzing the time evolution of a shielding current density  $\mathbf{j}$  in an HTS film containing a crack.

Throughout the present study, the geometrical and physical parameters are fixed as follows:  $a = 20$  mm,  $b = 600$  nm,  $E_c = 1$  mV/m,  $j_c = 1$  MA/cm<sup>2</sup>,  $N = 20$ ,  $R = 2.5$  mm,  $L = 0.5$  mm,  $M = 400$ , and  $f = 1$  kHz.

### 3. Numerical Results

In this section, we simulate the inductive method by using the numerical code. In the subsections 3.1 and 3.2,

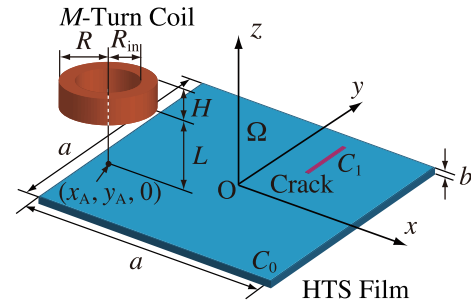


Fig. 1 A schematic view of an inductive method.

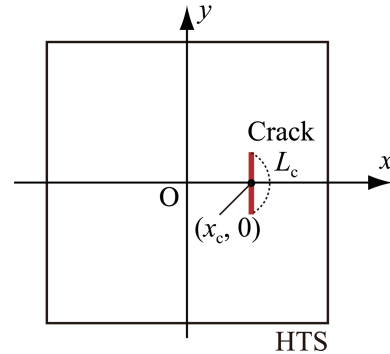


Fig. 2 A crack in an HTS film.

we assume an HTS film without a crack, and we take into account the crack in the subsection 3.3. A crack shape is a line segment with the center points  $(x, y) = (x_c, 0)$  in the  $xy$ -plane (see Fig. 2). The crack size  $L_c$  is given by  $L_c = 3.2$  mm.

#### 3.1 Mawatari's theory

According to Mawatari's theory [2], a critical current density  $j_c$  can be easily calculated from

$$j_c = 2F(r_{\max})I_T/b. \quad (5)$$

Here,  $F(r_{\max})$  is the maximum value of a primary coil-factor function  $F(x)$  [3] determined from the configuration of the coil and the HTS. In addition,  $I_T$  is a lower limit of the coil current  $I_0$  when a third-harmonic voltage  $V_3$  begins to develop in the coil. An important point is that (5) is also applicable only to an HTS film without any cracks.

In order to determine  $j_c$ , it is necessary to evaluate a threshold current  $I_T$  when a third-harmonic voltage  $V_3$  begins to develop in the coil. Since it is difficult to determine  $I_T$  accurately, we use the conventional voltage criterion [3]

$$V_3 = 0.1 \text{ mV} \Leftrightarrow I_0 = I_T^*. \quad (6)$$

Hence, we get an estimated value  $I_T^*$  of the threshold current  $I_T$ .

The third-harmonic voltage  $V_3$  is calculated as a function  $I_0$  and is depicted in Fig. 3. We see from this figure that  $V_3$  gradually develops above the certain value of  $I_0$ . By applying the voltage criterion (6) to the resulting  $I_0$ - $V_3$

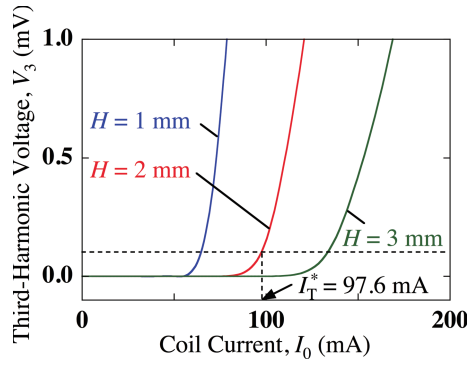


Fig. 3  $I_0$ - $V_3$  curves for  $R_{in} = 1.25$  mm. Here,  $x_A = y_A = 0$  mm.

curves, we obtain  $I_T^* = 64.4$  mA, 97.6 mA, and 133.9 mA for  $H = 1$  mm, 2 mm, and 3 mm, respectively.

### 3.2 Influence of coil shape on accuracy

In this subsection, we investigate the influence of the coil shape on the accuracy of the inductive method. For this purpose, we change the inner radius  $R_{in}$  or the height  $H$  of the coil. In addition, as a measure of the accuracy, we define a relative error

$$\varepsilon_r \equiv |I_T^* - I_T^A|/I_T^A. \quad (7)$$

Here,  $I_T^A$  is an analytic value of  $I_T$ , and it is defined by  $I_T^A \equiv j_c b / [2F(r_{max})]$ .

In Fig. 4, we show the dependence of the relative error  $\varepsilon_r$  on the height  $H$ . We see from this figure that the relative error  $\varepsilon_r$  monotonously increases with the height  $H$ . This is mainly because the slope of the tangent at the threshold current  $I_T^*$  becomes gently when  $H$  increases. However, when the height  $H$  is too small, it is not preferable in the fabrication of the coil.

In Fig. 5, we show the dependence of the relative error  $\varepsilon_r$  on the inner radius  $R_{in}$ . This figure indicates that  $\varepsilon_r$  decreases with  $R_{in}$  for  $R_{in} \leq 1.25$  mm, whereas, for  $R_{in} > 1.25$  mm, its value increases with  $R_{in}$  except for  $R_{in} = 1.5$  mm. Especially, it is found that the accuracy of the inductive method is highest at  $R_{in} = 1.25$  mm.

These results imply that it is preferred to reduce as much as possible the height of the coil. Moreover, It is found that the accuracy of is slightly improved by changing the inner radius, and there exists an optimum radius. In the following, the inner radius  $R_{in}$  and the height  $H$  are given by  $R_{in} = 1.25$  mm and  $H = 2$  mm.

### 3.3 Crack detection

Let us first investigate how a crack affects the estimated value  $I_T^*$  of the threshold current  $I_T$ . In Fig. 6, we show the  $I_0$ - $V_3$  curves for various  $x_A$ . By applying the voltage criterion to the  $I_0$ - $V_3$  curves, we get  $I_T^* = 97.6$  mA, 52.5 mA, and 33.1 mA for  $x_A = 1$  mm, 5 mm, and 9 mm, respectively. Incidentally, the analytic value  $I_T^A$  is  $I_T^A = 92.1$  mA. Compared with these values for  $x_A = 1$  mm, since

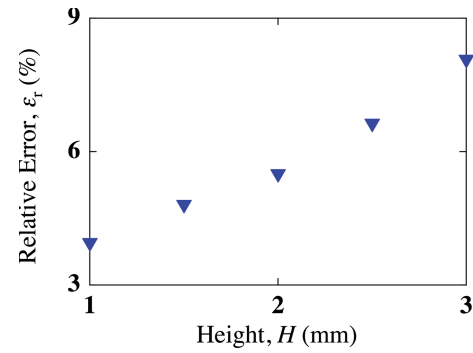


Fig. 4 Dependence of the relative error  $\varepsilon_r$  on the height  $H$  for  $R_{in} = 1.25$  mm. Here,  $x_A = y_A = 0$  mm.

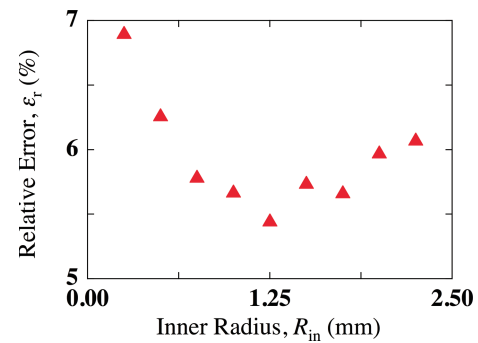


Fig. 5 Dependence of the relative error  $\varepsilon_r$  on the inner radius  $R_{in}$  for  $H = 2$  mm. Here,  $x_A = y_A = 0$  mm.

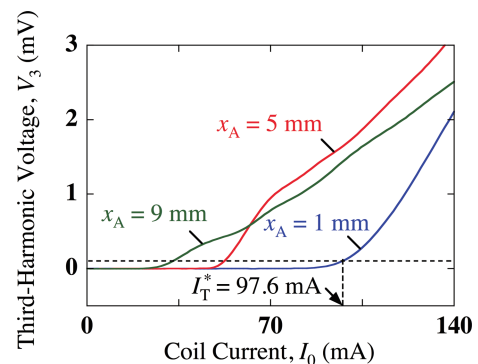


Fig. 6  $I_0$ - $V_3$  curves for  $x_c = 4$  mm.

the accuracy of the inductive method becomes high, the value of  $I_T^A$  almost agrees with  $I_T^*$ . On the other hand, the accuracy is remarkably degraded for  $x_A = 5$  mm and 9 mm. This is mainly because the orthographic projection of the coil overlaps with the crack or the film edge, and the spatial distribution of shielding current density  $\mathbf{j}$  is asymmetric about the symmetry axis of the coil (see Fig. 7).

Next, let us investigate the influence of the film edge on the crack detection. To this end, as a measure of the accuracy, we define another relative error

$$\varepsilon \equiv |I_T^{\max} - I_T^*|/I_T^{\max}. \quad (8)$$

Here,  $I_T^{\max}$  is denoted by  $I_T^{\max} = \max_{(x_A, y_A) \in \Omega} I_T^*(x_A, y_A)$ . Here-

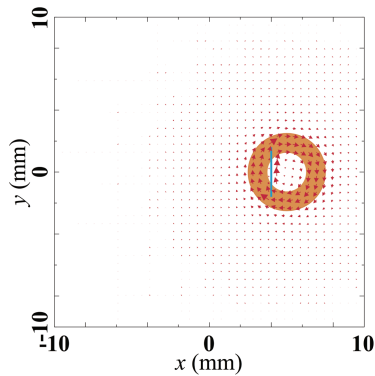


Fig. 7 Spatial distribution of the shield current density  $j$  for  $I_0 = I_T$  at time  $ft = 1.2$ . Here,  $x_A = 5$  mm and  $x_c = 4$  mm.

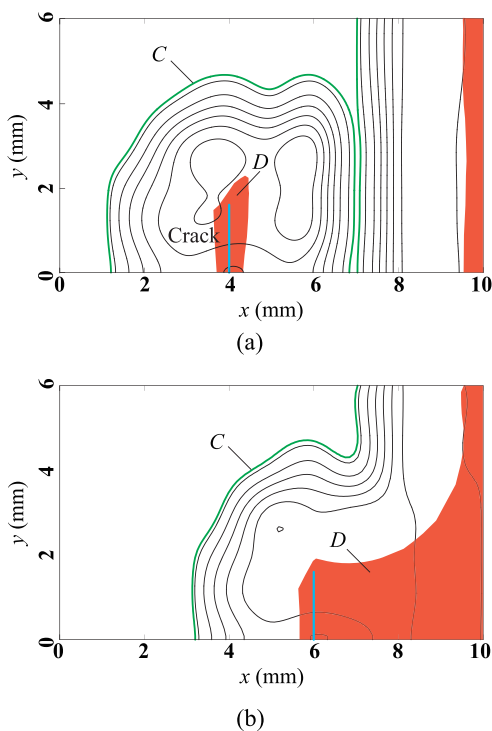


Fig. 8 Contour lines of the relative error  $\varepsilon$  for (a)  $x_c = 4$  mm and (b)  $x_c = 6$  mm. The green line  $C$  is the contour line of  $\varepsilon = 7\%$ .

after, in order to evaluate the spatial distribution of the relative error  $\varepsilon$ , we calculate the threshold current  $I_T^*$  at each measurement points in  $\Omega$ .

In Figs. 8 (a) and (b), we show the contour lines of the relative error  $\varepsilon$  for the case with  $x_c = 4$  mm and  $x_c = 6$  mm, respectively. In these figures, a tolerance error  $\varepsilon = 7\%$  is depicted by the green thick line  $C$ . In addition, the region  $D$  is depicted by the red shaded region. By using the outer radius  $R$  of the coil and the curve  $C$ , we determine a defect region  $D$ . The reason for using the radius  $R$  is because the resolution of the induction method is the outer diameter  $2R$ . Incidentally, the  $D$ -evaluation method is described in [6].

From Fig. 8 (a), two types of the region  $D$  can be ob-

tained. One is a small region containing the crack. The other is a region near the film edge. In contrast, it is found that a region in Fig. 8 (b) becomes large as compared with Fig. 8 (a). Consequently, the crack located near the film edge cannot be detected with high accuracy because the crack is treated the same as the film edge.

## 4. Conclusion

We have developed a numerical code analyzing the time evolution of the shielding current density in an HTS film containing a crack. By using the code, reproducing the inductive method numerically, we assess the influence of a coil shape on the accuracy of the inductive method. In addition, we investigate the influence of the film edge on the crack detection. Conclusions obtained in the present study are summarized as follows:

1. The accuracy of the inductive method is degraded with increasing the height of the coil. This result implies that it is preferred to reduce as much as possible the height. In addition, it is found that the accuracy is slightly improved by changing the inner radius of the coil, and there exists an optimum radius.
2. The crack located near the film edge cannot be detected with high accuracy because the crack is treated the same as the film edge.

For multiple cracks, the number of boundary conditions (4) and (5) increases with the number of cracks. In the future, we will analyze the time evolution of the shielding current density in an HTS containing multiple cracks, and we will numerically investigate the performance of the inductive method in those cases.

## Acknowledgment

This study was supported in part by pan Society for the Promotion of Science under a Grant-in-Aid for Scientific Research ((C) No.24560321). A part of this study was also carried out with the support and under the auspices of the National Institute for Fusion Science (NIFS) Collaboration Research program (NIFS13KNTS025, NIFS13KNXN267). Also, the Numerical computations were carried out on Hitachi SR16000 XM1 of the LHD Numerical Analysis Server in NIFS.

- [1] B.P. Martins, *Recent Developments in Superconductivity Research* (Nova Publishers, New York, 2006) p. 68.
- [2] J.H. Claassen, M.E. Reeves and R.J. Soulen, Jr., *Rev. Sci. Instrum.* **62**, 996 (1991).
- [3] Y. Mawatari, H. Yamasaki and Y. Nakagawa, *Appl. Phys. Lett.* **81**, 2424 (2002).
- [4] S.B. Kim, *Physica C* **463-465**, 702 (2007).
- [5] A. Kamitani and S. Ohshima, *IEICE Trans. Electron.* **E82-C**, 766 (1999).
- [6] A. Kamitani, T. Takayama and S. Ikuno, *Physica C.* **494**, 168 (2013).